Electronic Supplementary Material (ESI) for Chemical Science.


# SUPPLEMENTARY INFORMATION

# Minimalistic Supramolecular Proteoglycan Mimics by Co-assembly of Aromatic Peptide and Carbohydrate Amphiphiles

Alexandra Brito[ab+], Yousef M. Abul-Haija[cd+], Diana S. Costa[ab], Ramon Novoa-Carballal[ab], Rui L. Reis[abe], Rein V. Ulijn[fgh*], Ricardo A. Pires[abe*], Iva Pashkuleva[ab*]

[a] 3B's Research Group, I3Bs – Research Institute on Biomaterials, Biodegradables and Biomimetics, University of Minho, Headquarters of the European Institute of Excellence on Tissue Engineering and Regenerative Medicine, AvePark, Parque de Ciência e Tecnologia, Zona Industrial da Gandra, 4805-017 Barco, Guimarães, Portugal. E-mail: pashkuleva@i3bs.uminho.pt; rpires@i3bs.uminho.pt

[b] ICVS/3Bs - PT Government Associate Laboratory, Braga/Guimarães, Portugal.

[c] Current Address: WestCHEM, School of Chemistry, University of Glasgow, Glasgow G12 8QQ, UK.

[d] Department of Pure and Applied Chemistry, University of Strathclyde, Glasgow G1 1XL, UK.

[e] The Discoveries Centre for Regenerative and Precision Medicine, Headquarters at University of Minho, Avepark, 4805-017 Barco, Guimarães, Portugal

[f] Advanced Science Research Center (ASRC) at the Graduate Center, City University of New York (CUNY), 85 St Nicholas Terrace, New York, New York 10031, USA. E-mail: rein.ulijn@asrc.cuny.edu

[g] Department of Chemistry, Hunter College, City University of New York, 695 Park Avenue, New York 10065, USA

[h] Ph.D. programs in Biochemistry and Chemistry, The Graduate Center of the City University of New York, New York 10016, USA

[+] These authors contributed equally to this work.

**S1. Synthesis of aromatic carbohydrate amphiphiles (CA)**

All commercial reagents were used without purification. The used solvents were analytical or HPLC grade.

Aromatic carbohydrate amphiphiles (1) were obtained from the respective glucosamines using previously reported one-step synthetic procedure (Fig. S1).1, 2 Briefly, sodium salt of glucosamine (GlcN, Carbosynth, UK) or its derivatives (6-sulfate glucosamine, GlcN6S or 6-phosphate glucosamine, GlcN6P, Carbosynth, UK) was dissolved in water (30 g/L) in the presence of 2 eq sodium hydrogen carbonate (Riedel-de Haen, Germany). The 9-Fluorenylmethoxycarbonyl chloride (Fmoc-Cl, Sigma, Germany, 1.5-2 eq.) was dissolved in 50 g/L of dioxane (Sigma, Germany) and added dropwise to the solution of the respective glucosamine. The reaction mixture was stirred at room temperature under nitrogen atmosphere during 48 h. The dioxane:water reaction mixture was frozen in liquid nitrogen and freeze-dried.

The obtained white powder was dissolved in water and a liquid-liquid extraction with diethyl ether was applied to remove the unreacted Fmoc-Cl. The water phase was collected and column chromatography (70-230 and 230-400 mesh silica gel) was performed to remove any remaining Fmoc-Cl and to separate the unreacted glucosamine from the product. The used eluent was EtOAc/MeOH/H2O (7/2/1) for the sulfate derivative and EtOAc/MeOH/H2O (5/3/2) for the phosphate one. The solvents were removed by rotary evaporator and the aqueous solution was freeze-dried to obtain the purified **1a-c** as a white powder (Yield **1a**: 76%, **1b**: 70%, **1c**: 81%). The structure and purity of the final products were confirmed by ESI-MS, NMR, and HPLC.

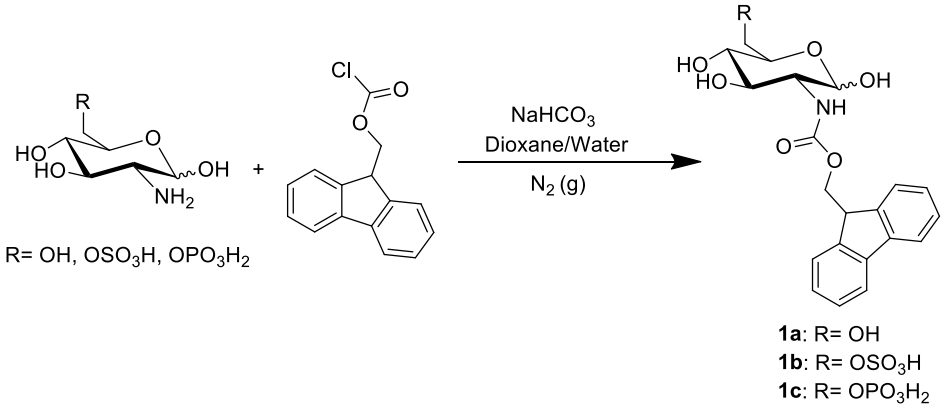


**Figure S1.** Synthesis of the aromatic carbohydrate amphiphiles.

## S2. Characterization of aromatic carbohydrate amphiphiles

The purity of the samples was determined by HPLC (KANUER, Germany) using a 250 mm x 4.6 mm reverse-phase C18 Atlantis column (Waters, UK), a flow of 1 mL/min, a UV detection wavelength at 280 nm and two buffers: A - water (with 0.1% trifluoroacetic acid, Sigma, Germany); and B - acetonitrile (VWR, with 0.1% trifluoroacetic acid). The HPLC runs comprised an initial step of 4 min under isocratic flow of 80% of buffer A, followed by a gradient to 80% of B at 31 min; this buffer composition (80% of B) was maintained for 5 min, followed by a gradient to 80% of A for 2 min and an isocratic elution (under 80% of A) during 4 min. $^{1}H$ and $^{13}C$ NMR spectra were recorded on Bruker Avance III spectrometer (Bruker, Gemrany) at 25 °C in $D_2O$. The chemical shifts are reported in ppm ($\delta$ units) downfield to the solvent signal. Duplicated signals observed for some protons and carbons correspond to the two anomeric forms. Mass spectra were acquired on an electrospray ionization (ESI) mass spectrometer (MS) Finnigan LXQ (Thermo Electron Corporation, USA) under negative-ion mode.

### S2.1. Fmoc-Glucosamine (Fmoc-GlcN, 1a)

$^{1}H$ NMR (400 MHz, DMSO-$d_6$, 298 K): $\delta$ 7.89-7.82 (dd, 2H, *J*= 8Hz; 12Hz, H'6); 7.74-7.71 (dd, 2H, *J*= 8Hz; 12Hz, H'3); 7.42-7.37 (m, 2H, H'5); 7.35-7.28 (m, 2H, H'4), 6.44 (s, 1H, OH), 4.97 (d, 1H, H'1), 4,94 (s, 1H, OH); 4.71 (s, 1H, OH), 4.43 (d, 1H, H'1'), 4.59-4.21 (m, 2H, H'2 + H4); 3.87-3.32 (m, 5H)

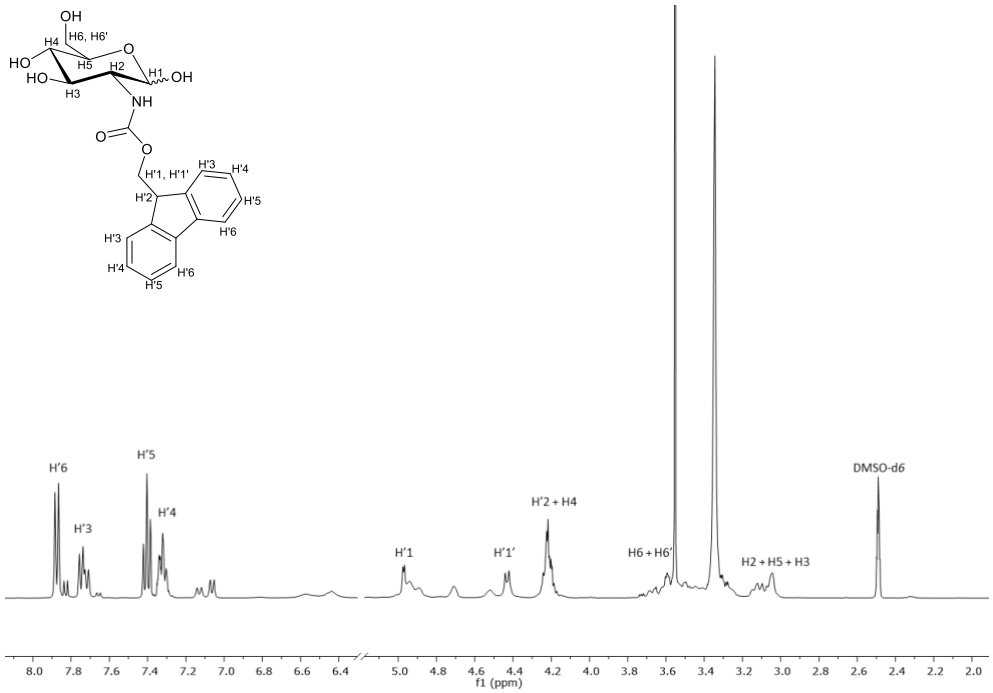


**Figure S2.** $^{1}H$ NMR (400 MHz, DMSO-$d_6$, 298 K) of Fmoc-GlcN (**1a**).

$^{13}$C NMR (75 MHz, DMSO-d$_6$, 298 K): δ (duplicated signals are observed for some carbons; asterisks indicate those corresponding to the alpha anomer) 156.16; 143.92 139.41; 137.42; 128.91; 127.30; 124.20; 121.38; 120.03; 90.80; 74.73; 71.03; 70.17; 68.55; 61.16; 59.12; 56.39.

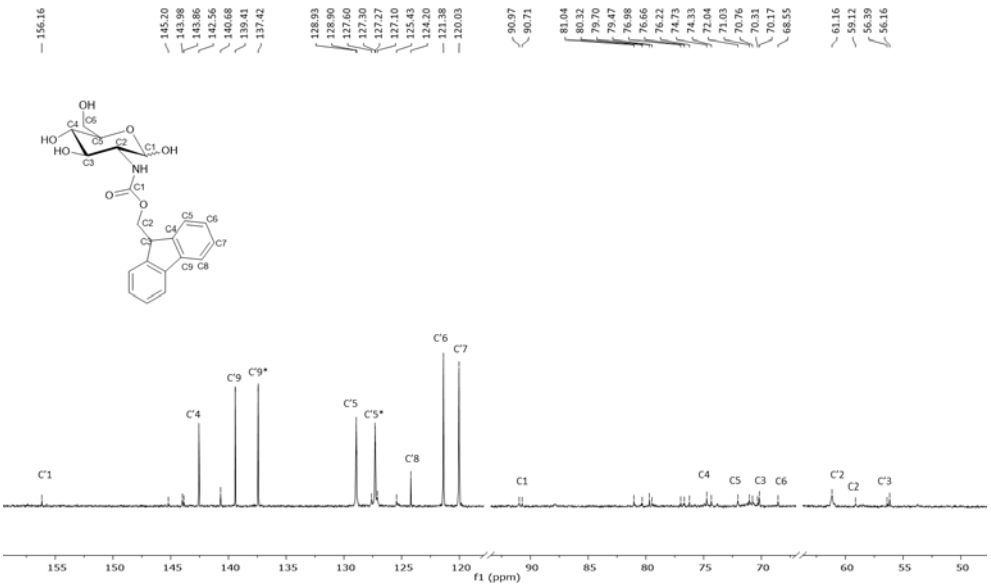


**Figure S3.** $^{13}$C NMR (75 MHz, DMSO-*d*$_6$, 298 K) of Fmoc-GlcN (**1a**).

HPLC characterization of purity of Fmoc-GlcN (**1a**).

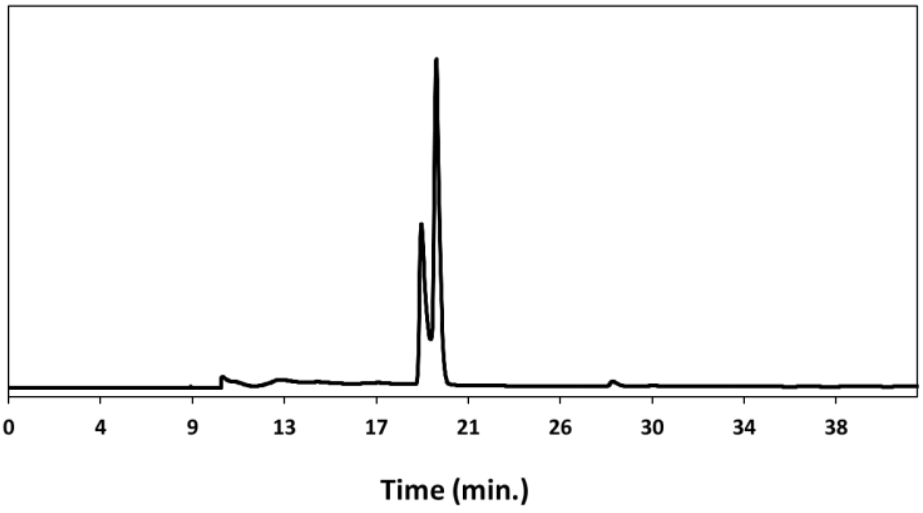


**Figure S4.** HPLC run of the purified Fmoc-GlcN (**1a**), showing the two anomers**.**

ESI-MS (*m/z*): $[M - Na]^+$ 424.39

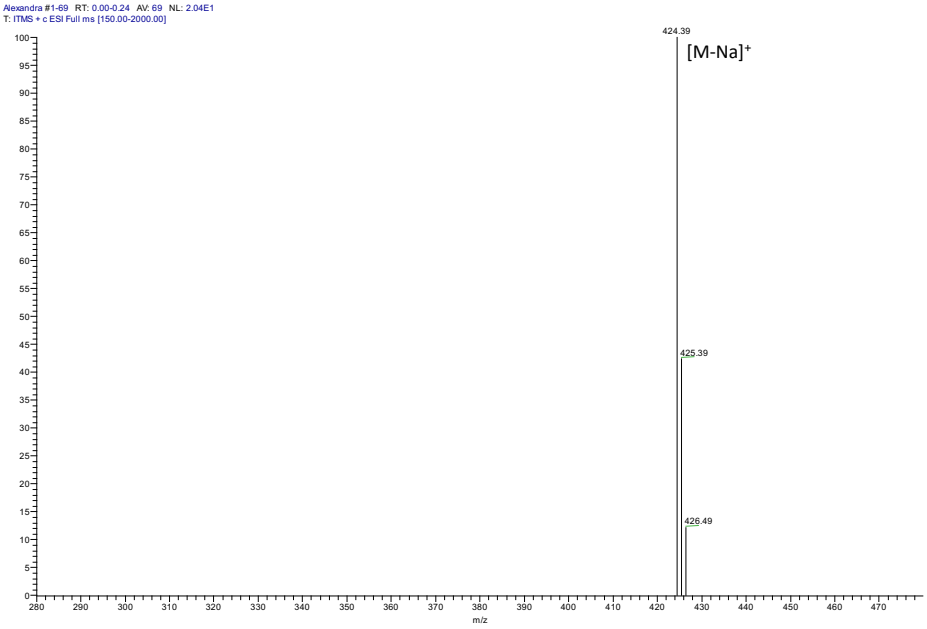


**Figure S5.** ESI-MS spectrum of Fmoc-GlcN (**1a**).

### S2.2. Fmoc-Glucosamine-6-O-sulfate (Fmoc-GlcN6S, 1b)

$^1$H NMR (400 MHz, $D_2O$, 298 K): 7.91-7.86 (dd, 2H, *J*= 8Hz; 12Hz, H'6); 7.77-7.68 (dd, 2H, *J*= 8Hz; 12Hz, H'3); 7.52-7.49 (m, 2H, H'5); 4.45-7.43 (m, 2H, H'4), 5.06* (s, 1H), 4.99 (s, 1H), 4,69 (m, 1H, H'1); 4.57 (m, 1H, H'1'), 4.31 (m, 2H, H6 + H6'), 4.01 (m, 1H, H2); 3.70 (m, 2H, H5 + H3). Asterisk indicates the alpha anomer.

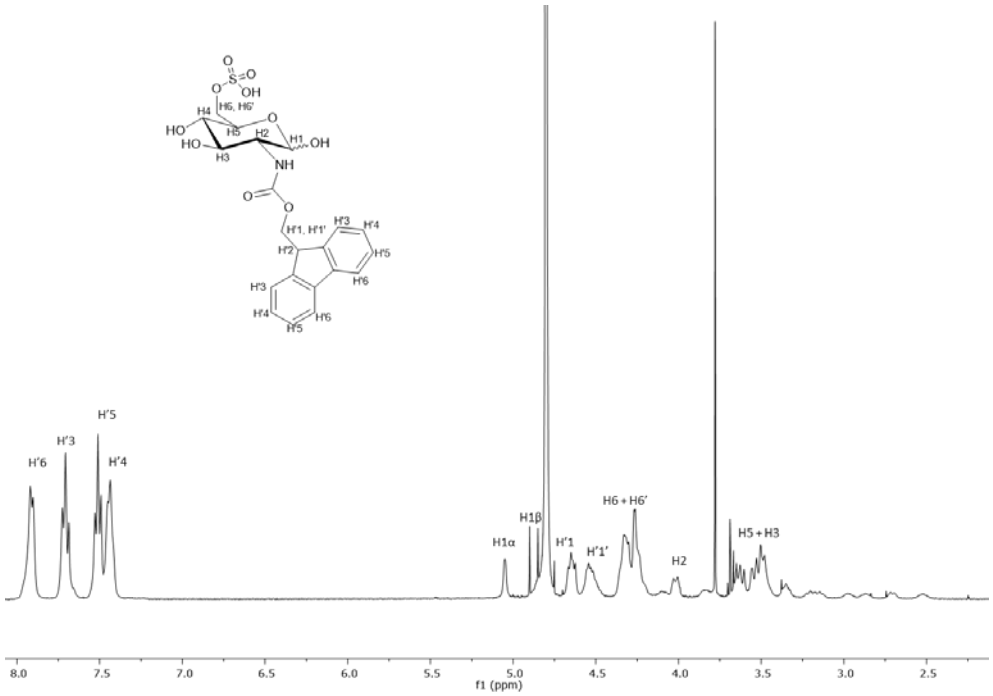


**Figure S6.** $^1$H NMR (400 MHz, $D_2O$, 298 K) of purified Fmoc-GlcN6S (**1b**).

$^{13}$C NMR (75 MHz, $D_2O$, 298 K): 158.04; 143.91; 140.92; 127.99; 127.45; 124.90; 120.11; 95.14; 91.22; 73.66; 70.84; 69.53; 67.13; 66.41; 62.51; 55.25.

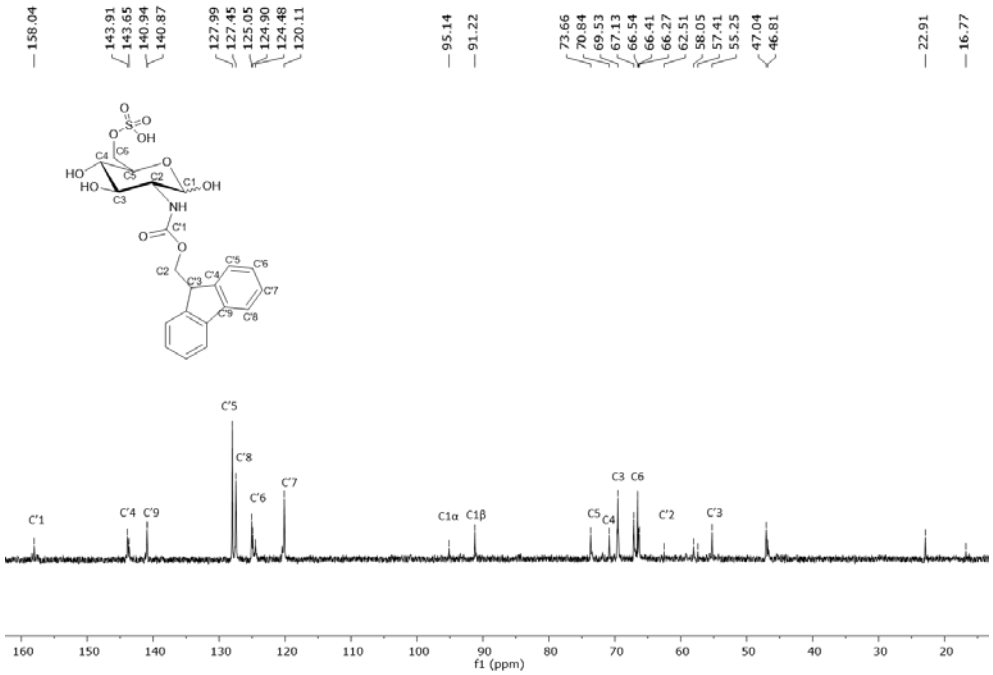


**Figure S7.** $^{13}$C NMR (75 MHz, $D_2O$, 298 K) of Fmoc-GlcN6S (**1b**)

HPLC characterization of purity of Fmoc-GlcN6S (**1b**).

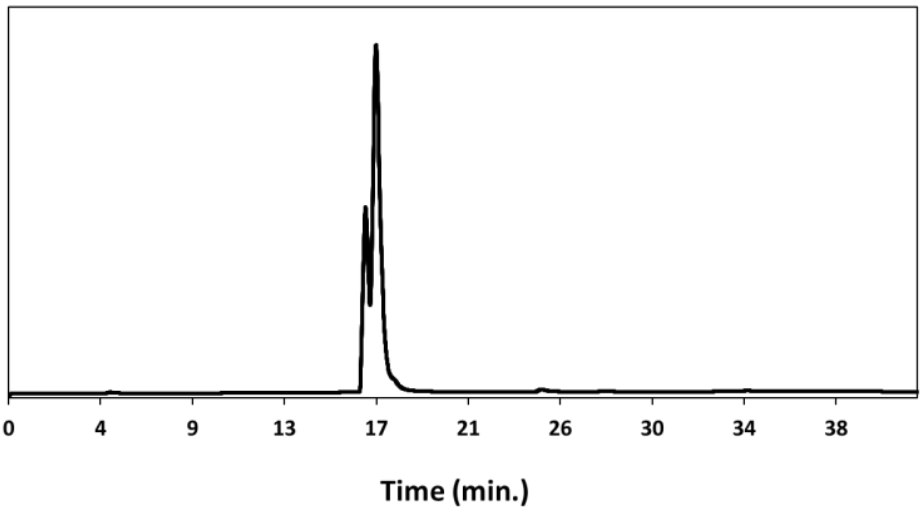


**Figure S8.** HPLC run of the purified Fmoc-GlcN6S (**1b**), showing the two anomers.

ESI-MS (*m/z*): [M - H]$^-$ 480.13

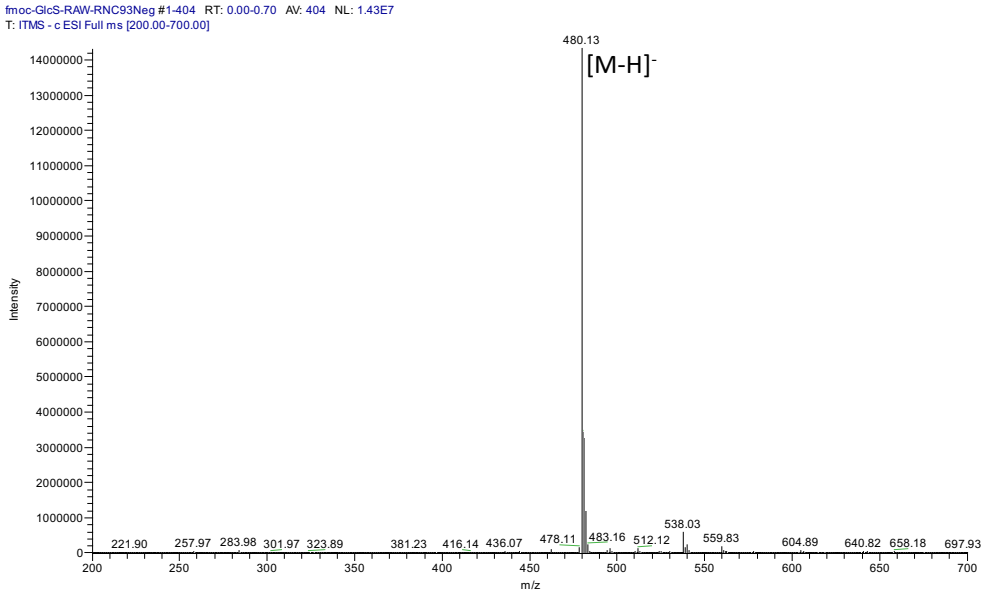


**Figure S9.** ESI-MS spectrum of Fmoc-GlcN6S (**1b**).

### S2.3. Fmoc-Glucosamine-6-O-phosphate (Fmoc-GlcN6P, 1c)

$^1$H NMR (400 MHz, $D_2O$, 298 K): 7.94-7.93 (dd, 2H, *J*= 8Hz; 12Hz, H'6); 7.74-7.71 (dd, 2H, *J*= 8Hz; 12Hz, H'3); 7.54-7.52 (m, 2H, H'5); 7.51-7.45 (m, 2H, H'4), 5.26* (s, 1H), 5.05 (s, 1H), 4,55 (m, 1H, H'1); 4.33 (m, 1H, H'1'), 4.12 (m, 2H, H6 + H6'), 4.06 (m, 1H, H2); 3.52 (m, 2H, H5 + H3).

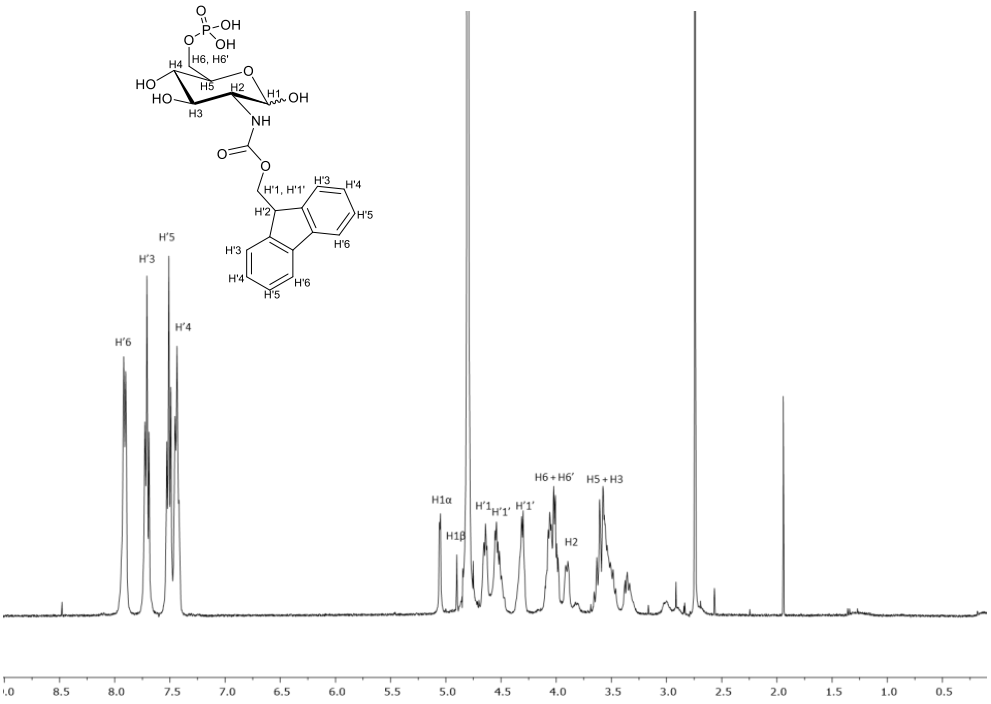


**Figure S10.** $^1$H NMR (400 MHz, $D_2O$, 298 K) of purified Fmoc-GlcN6P (**1c**).

$^{13}$C NMR (75 MHz, $D_2O$, 298 K): δ 158.08; 143.88; 140.92; 128.02; 127.48; 124.99; 120.13; 91.23; 89.25; 71.75; 69.45; 69.10; 66.27; 63.25; 55.37.

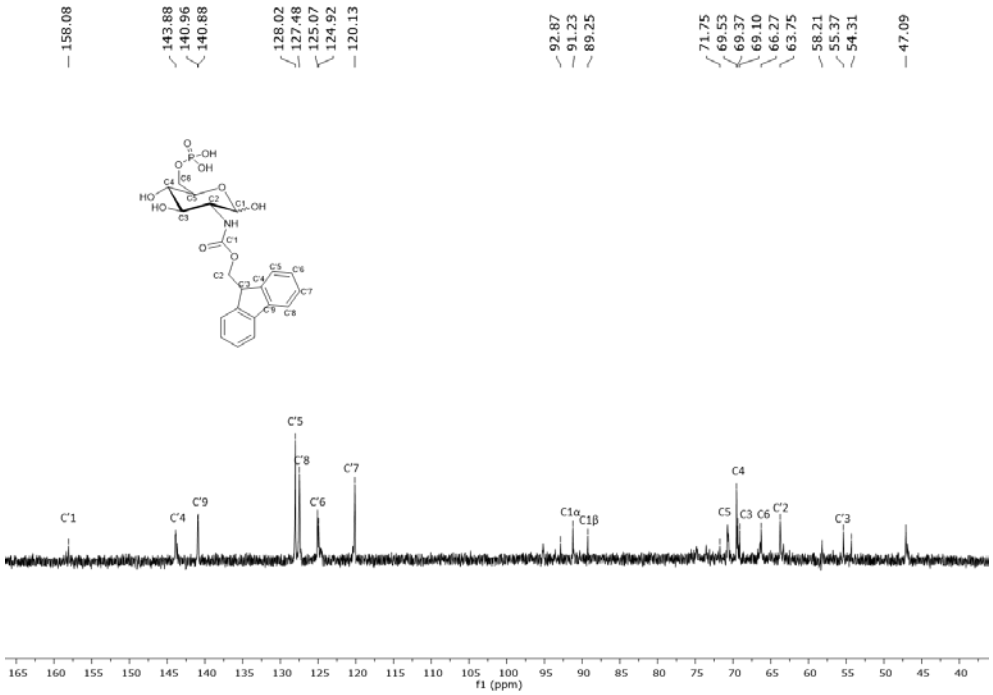


**Figure S11.** $^{13}$C NMR (75 MHz, $D_2O$, 298 K) of Fmoc-GlcN6P (**1c**)

HPLC characterization of purity of Fmoc-GlcN6P (**1c**).

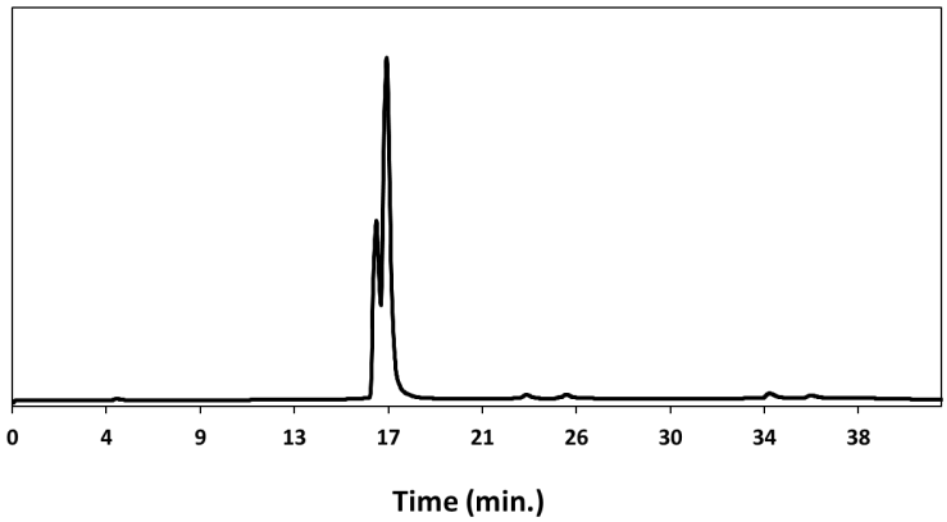


**Figure S12.** HPLC run of the purified Fmoc-GlcN6P (**1c**), showing the two anomers.

ESI-MS (m/z): $[M - H]^-$ 480.08

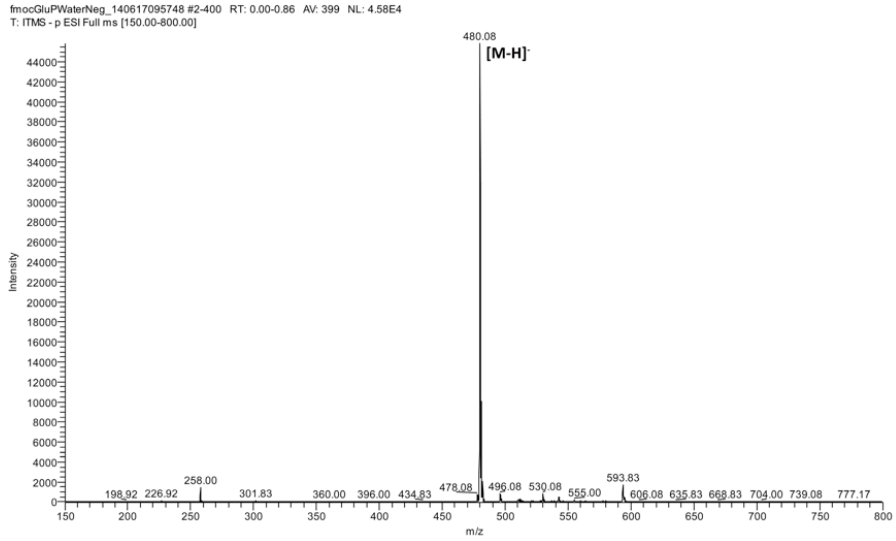


**Figure S13.** ESI-MS spectrum of Fmoc-GlcN6P (**1c**).

**S3. Self-assembly of aromatic carbohydrate amphiphiles (1) and Fmoc-FF (2)**

Single component solutions were prepared by dissolving each of the components (**1** and **2**) in water. Fmoc-GlcN (10 mM, **1a**) dissolved only upon temperature increase to 80 °C as previously reported.[2] Formation of translucent hydrogel was observed when the obtained solution was cooled down to room temperature. A transparent solution of Fmoc-FF (BiogelX, 10 mM, **2**) was obtained after rising the pH to 11-11.5 (0.5 M NaOH).[3] The pH of this solution was then adjusted to 8 (0.5 M HCl), filtered (0.8 μm syringe filters) and stored at 4 °C for 24 h. No additional adjustments were needed to dissolve Fmoc-GlcN6S (5 mM, **1b**) and Fmoc-GlcN6P (5 mM, **1c**). Each single component solution was characterized by atomic force microscopy (AFM).

Co-assembly of Fmoc-FF and Fmoc-GlcN6X (X=S or P) was studied at room temperature. Samples were prepared by suspending Fmoc-FF (10 mM) and Fmoc-GlcN6X at different concentrations (2.5, 5 and 10 mM) in water. A complete dissolution was achieved for the systems obtained with 2.5 and 5 mM Fmoc-GlcN6X by adding 0.5 M NaOH (pH 11) to the obtained suspension and then vortexing it (Fig. S14). After decreasing the pH to 8 (0.5 M HCl), the solutions were filtered (0.8 μm syringe filters) and characterized by circular dichroism (CD) and fluorescence emission spectroscopy. All results described in the main manuscript were performed with the system Fmoc-FF (10 mM)/Fmoc-GlcN6X (5 mM).

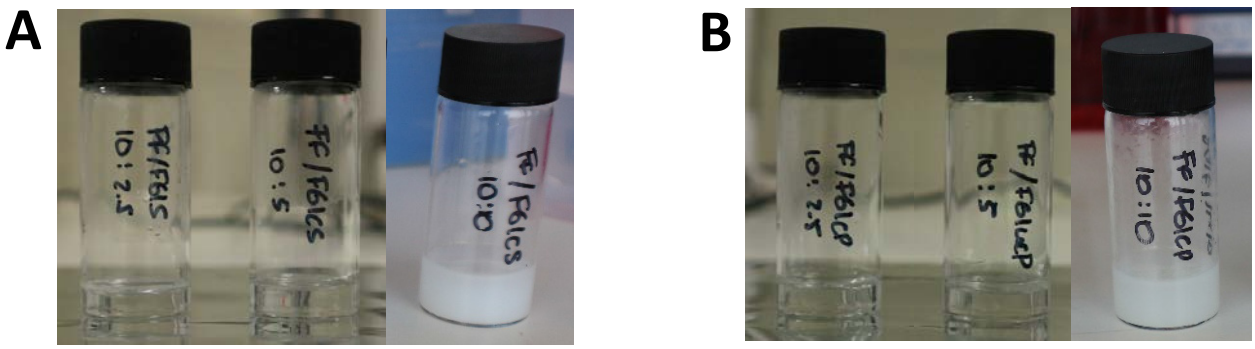


**Figure S14.** Water solutions of 10 mM Fmoc-FF (**2**) with either (A) Fmoc-GlcN6S (**1b**) or (B) Fmoc-GlcN6S (**1b**) at concentrations 2.5, 5 and 10 mM.

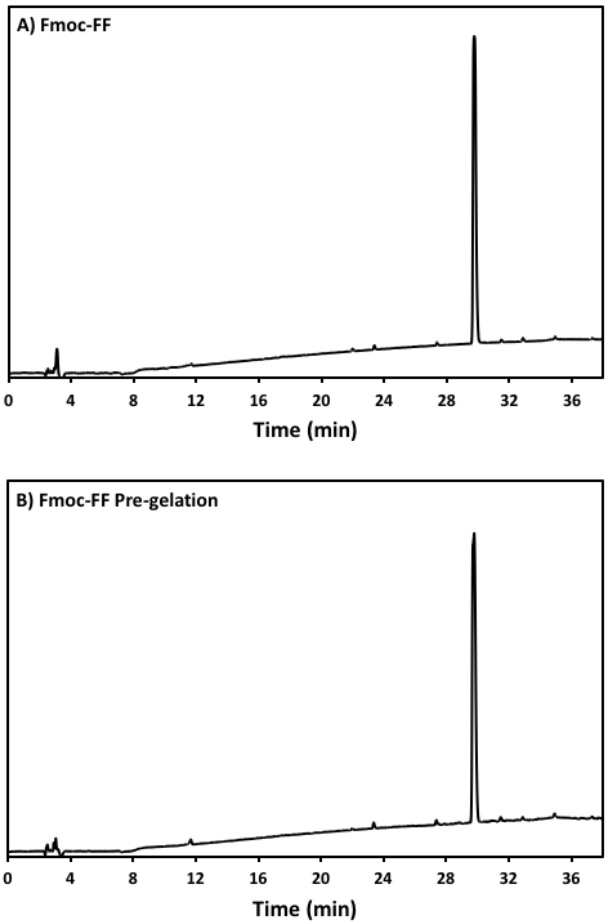


**Figure S15.** HPLC runs of Fmoc-FF before (A) and after (B) solubilization in water using basic pH. No fmoc cleavage was observed after the solubilization.

### S3.1. Atomic force microscopy (AFM)

(3-Aminopropyl)triethoxysilane (APTES, 200 µL) was dropped on a fresh cleaved mica sheet and let for 30 min at room temperature. Then, the mica was rinsed with deionized water and dry under nitrogen flow. A drop of the above described solutions of CA, PA and CA/PA was deposited on the functionalized mica sheet. AFM images were acquired with a JPK Nanowizard 3 in air at room temperature under AC mode. The scans were acquired at 512 x 512 pixels resolution using ACTA-SS probes (k~37 N/m, AppNano, USA), a drive frequency 254 kHz, setpoint 0.5 V and a scanning speed 1.0 Hz. Images were analyzed using the JPK data processing software. The mechanical properties of the nanofibers were determined under JPK quantitative imaging mode using TAP525 probes (k~200 N/m, Bruker, Germany) calibrated by the contact free method. Approaching force curves were fitted using Hertz model to obtain the elastic modulus (E). The reported E is averaged over 30 measurements.

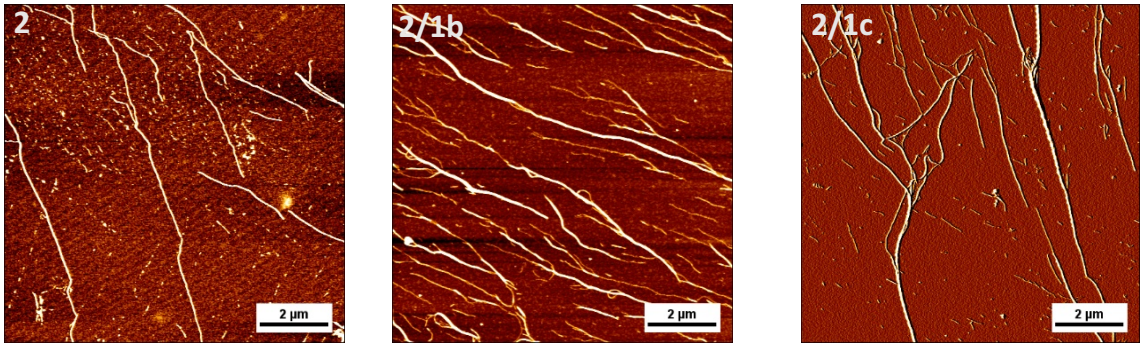


**Figure S16.** Supplementary AFM images for the studied systems. The used concentrations were 10 mM for (**2**) and 5 mM for (**1b**) and (**1c**).

**Table S1.** Dimensions (determined by AFM) and zeta potential (determined by dynamic light scattering, DLS) of single and bi-component fibers

| Components | Fiber height [nm] | Fiber width [nm] | ζ-Potential [mV] |
|---|---|---|---|
| Fmoc-FF | 2.8 ± 0.5 | 20.6 ± 2.2 | 0.0 ± 0.0 |
| Fmoc-GlcN | 4.6 ± 1.3 | 19.0 ± 3.1 | --* |
| Fmoc-FF/Fmoc-GlcN6S | 9.1 ± 1.1 | 51.1 ± 12.5 | -56.0 ± 1.5 |
| Fmoc-FF/Fmoc-GlcN6P | 5.4 ± 1.2 | 35.1 ± 2.9 | -55.4 ± 6.1 |

* Limited solubility

### S3.2 Zeta Potential

The zeta potential of pre-gelation solutions was measured by Nano ZS (Malvern Instruments, Malvern, UK). The mobility of nanostructures was measured and was converted to zeta potential by the software. Size of the assemblies generated from carbohydrate amphiphiles **1b** and **1c** (single component systems) was also determined using this equipment. The measurements were taken after 24 h of sample preparation.

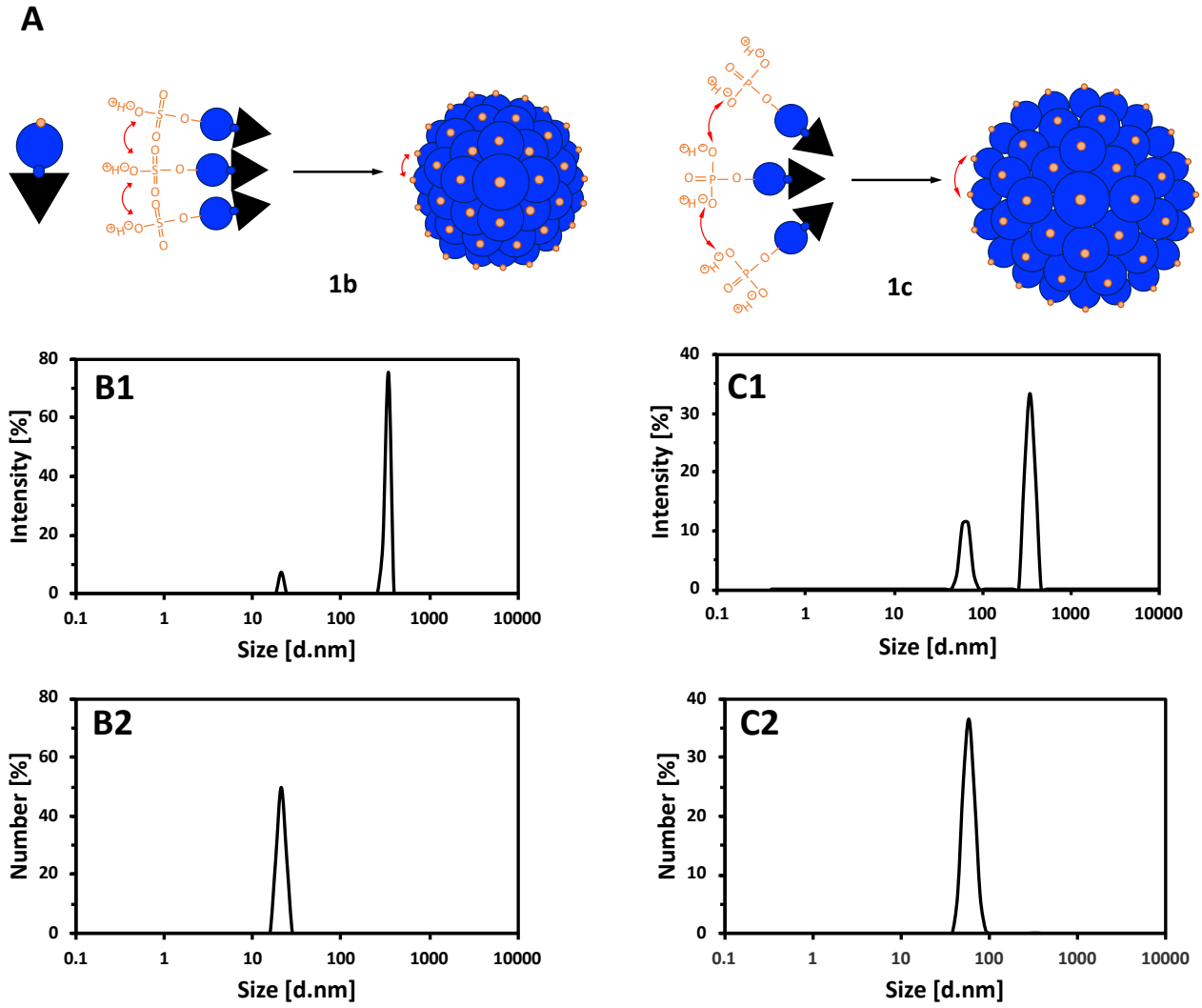


**Figure S17.** Schematic presentation (A) and dynamic light scattering data about size for single component assemblies in water of **1b** (B) and **1c** (C) at concentration 10 mM. The intensity distribution (B1 and C1) showed presence of aggregates but the number distribution (B2 and C2) and the polydispersive index (PDI: 0.5 for **1b** and 0.4 for **1c**) indicated that their concentration is relatively low.

### S3.3 Circular dichroism (CD)

40 μL of each amphiphile(s) solution were analyzed using a cuvette of 1 mm pathlength. CD spectra were acquired at 37 °C on a Jasco J-810 spectrometer within the range of 200-400 nm using a bandwidth of 1 nm. Each spectrum was obtained by accumulation of three acquisitions.

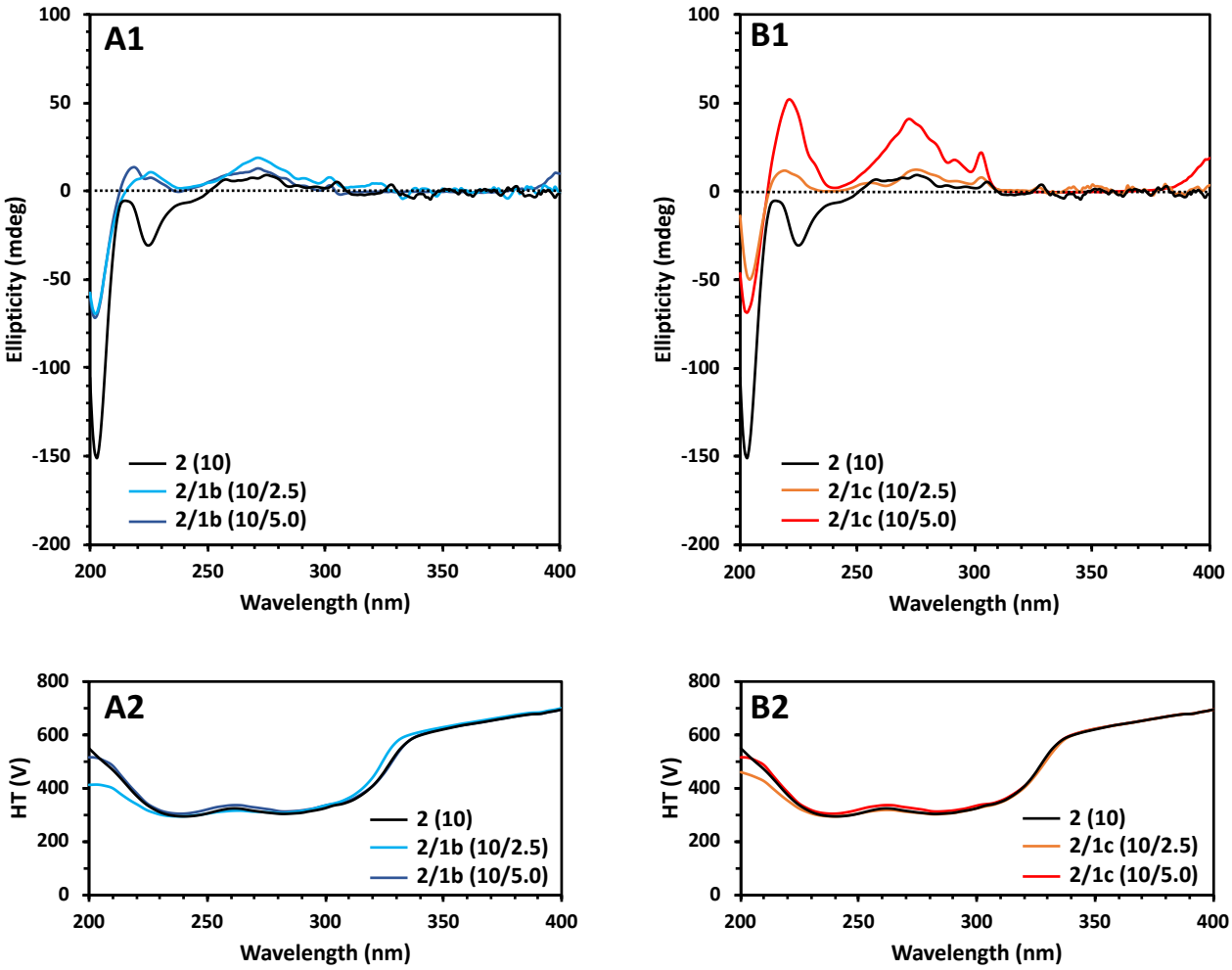


**Figure S18**. CD (A1, B1) and HT (A2, B2) spectra of the peptide amphiphile Fmoc-FF (**2,** 10 mM) and its co-assemblies with carbohydrate analogues GlcN6S (**1b**) and GlcN6P (**1c**) at different ratios.

### S3.4 Fluorescence emission spectroscopy

Fluorescence emission spectra were recorded within the range 300-600 nm using a Jasco FP-6500 spectrofluorimeter. An excitation wavelength of 295 nm and a slit width of 3 nm was used. The data are presented as an average of three measurements.

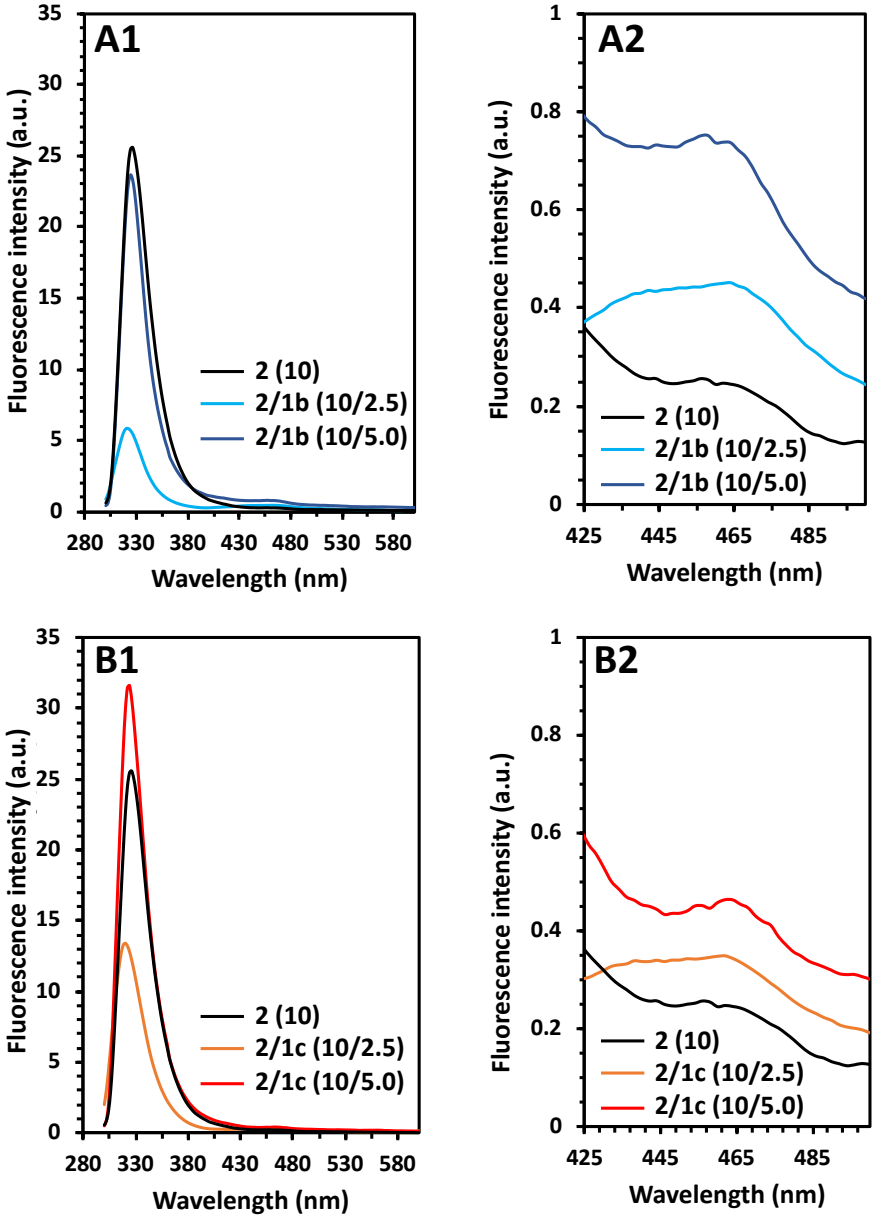


**Figure S19.** Fluorescence spectra of solutions of Fmoc-FF (**2,** 10 mM) and its mixtures (A) Fmoc-FF/Fmoc-GlcN6S (**2**/**1b**) and (B) Fmoc-FF/Fmoc-GlcN6P (**2**/**1c**) at different ratios.

### S3.5 Transmission electron microscopy

Carbon-coated copper grids (200 mesh) were glow discharged in air for 30 s. The support film was touched onto the gel surface for 3 s and blotted down using filter paper. Negative stain (20 mL, 1% aqueous methylamine vanadate obtained from Nanovan; Nanoprobes) was applied and the mixture blotted again using filter paper to remove excess. The dried specimens were then imaged using a LEO 912 energy filtering transmission electron microscope operating at 120kV fitted with 14 bit/2 K Proscan CCD camera.

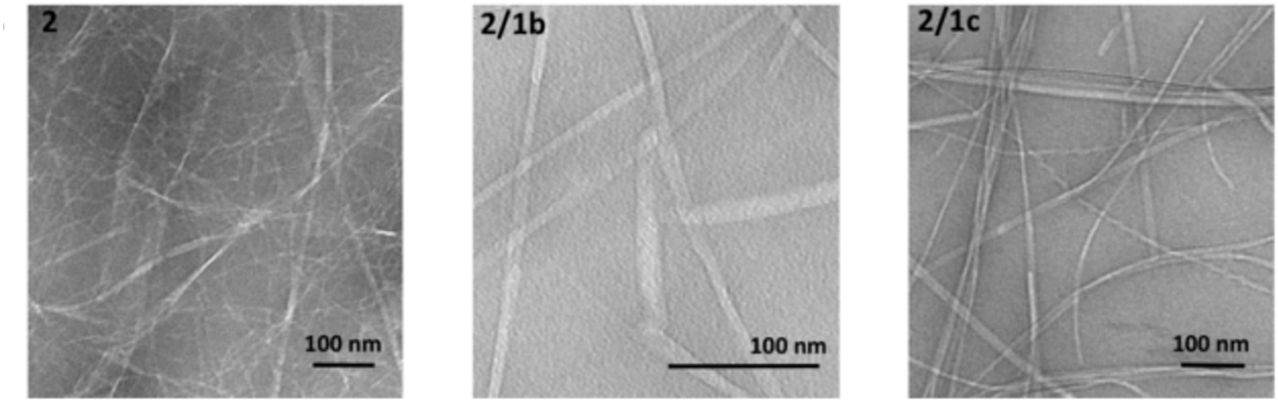


**Figure S20.** TEM images of the fibers obtained by self-assembly of the Fmoc-FF (**2**, 10 mM) and its co-assemblies with the carbohydrate amphiphiles Fmoc-GlcN6S (**1b**, 5 mM) and Fmoc-GlcN6P (**1c**, 5 mM).

### S3.6 Fourier transform infrared spectroscopy

Spectra were acquired using a Bruker Vertex 70 spectrometer with a spectral resolution of 1 $cm^{-1}$. The spectra were obtained by averaging 25 scans per sample. Measurements were performed in a standard IR cuvette (Harrick Scientific), in which the sample was contained between two $CaF_2$ windows (thickness, 2 mm) separated by a 25 μm PTFE spacer. All sample manipulations were performed in a glove box to minimize interference from atmospheric water vapour. $D_2O$ (Sigma-Aldrich) was used as the solvent for all the infrared spectral measurements.

### S4. Preparation and characterization of the hydrogels

The single component Fmoc-FF hydrogel and its co-assemblies Fmoc-FF/Fmoc-GlcN6S and Fmoc-FF/Fmoc-GlcN6P were prepared using identical protocol. Briefly, the water solutions described above were mixed with a pipette carefully to homogenize them and to remove any air bubbles. 500 μL of each solution was pipetted into transwell cell culture insert (12 wells, Greiner Bio-one), placed into 12 wells culture plate and 1.5 mL of cell culture medium (Dulbecco's Modified Eagle's Medium, DMEM) was added into the well. The plate was placed in an incubator (37 °C, humidified atmosphere of 5% $CO_2$, 2 h) to complete the gelation process. After this period, the medium was refreshed and additional 200 μL DMEM were gently pipetted on top of the gel.

As Fmoc-GlcN is not soluble at room temperature the gels Fmoc-FF/Fmoc-GlcN were prepared following a different procedure. A solution of Fmoc-FF (10 mM) in water was prepared as described above. Then, Fmoc-GlcN (5 mM) was added to this solution, the temperature was raised to 80 °C and stirred for 1 h. The obtained clear solution was allowed to cool at room temperature and hydrogelation was assessed by inversion of the reaction vial.

### S4.1. Atomic force microscopy

AFM images were acquired with a JPK Nanowizard 3 in air at room temperature under AC mode. The scans were taken at 512 x 512 pixels resolution using ACTA-SS probes (k~37 N/m, AppNano, USA), a drive frequency 317 kHz, setpoint 0.6 V and a scanning speed 0.5 Hz. Images were analyzed using JPK data processing software.

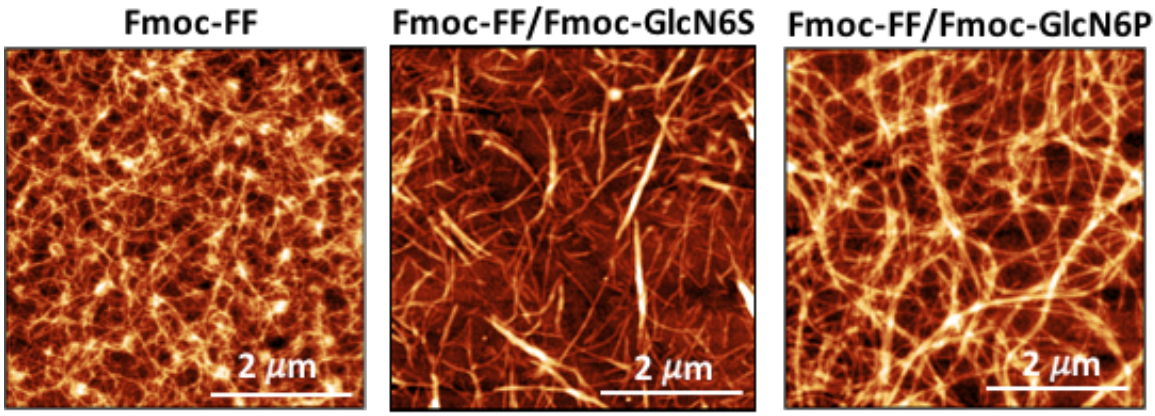


**Figure S21.** Supplementary AFM images for the supramolecular hydrogels obtained by assembly of Fmoc-FF (**2**, 10 mM), Fmoc-FF/Fmoc-GlcN6S (**2/1b**, 10 mM/5 mM) and Fmoc-FF/Fmoc-GlcN6P (**2/1c,** 10 mM/5 mM).

### S4.2. Rheometry

The mechanical properties of the hydrogels were measured on a Kinexus Rheometer with an 8 mm/cone-plate geometry. The elastic (G') and viscous (G'') moduli of the hydrogels were recorded as a function of frequency between 0.01 and 10 Hz. A solvent trap was used to keep the sample hydrated and the temperature of the sample was maintained at 37 °C by an integrated temperature controller.

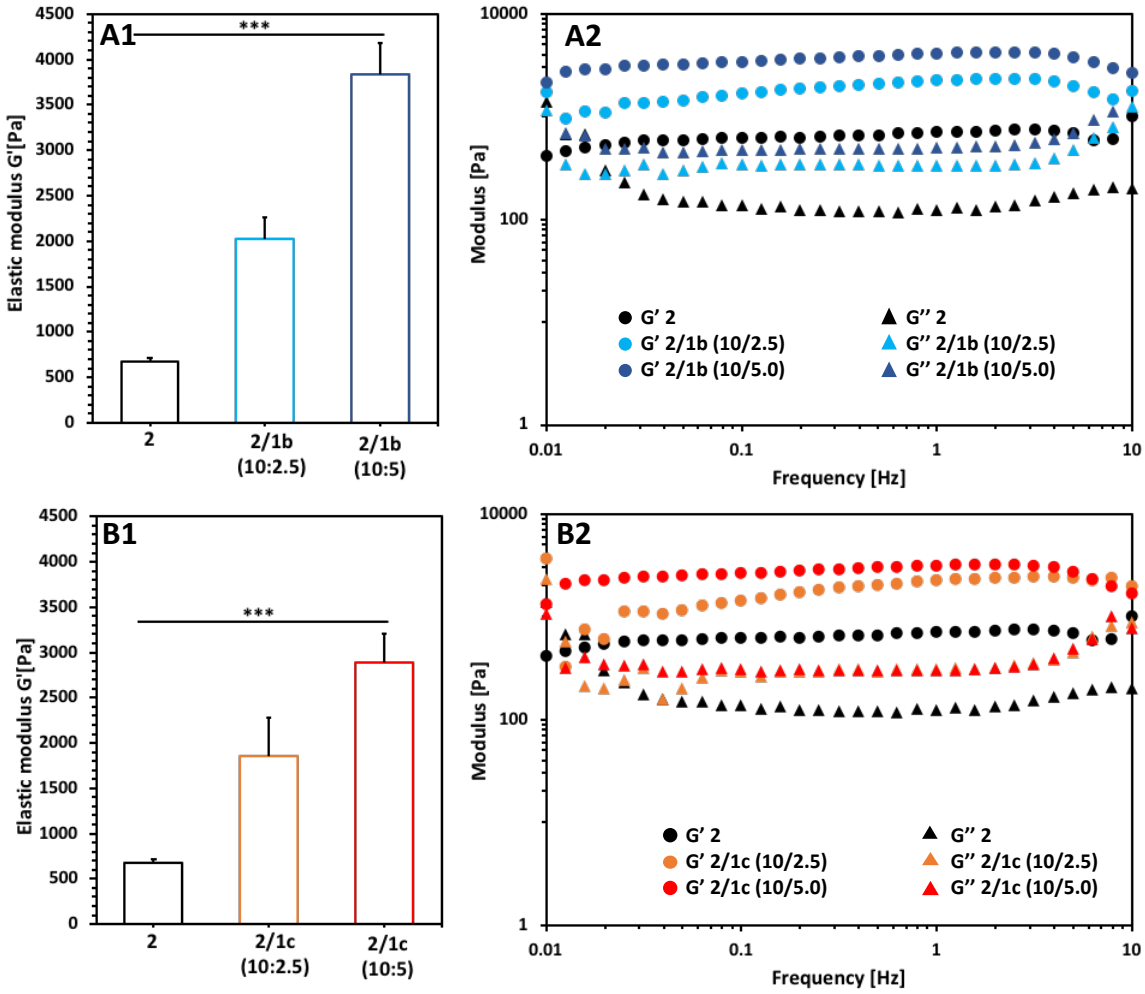


**Figure S22.** Rheology data illustrating the effect of carbohydrate amphiphiles (A) Fmoc-GlcN6S (**1b**) and (B) Fmoc-GlcN6P (**1c**) on gel stiffness.

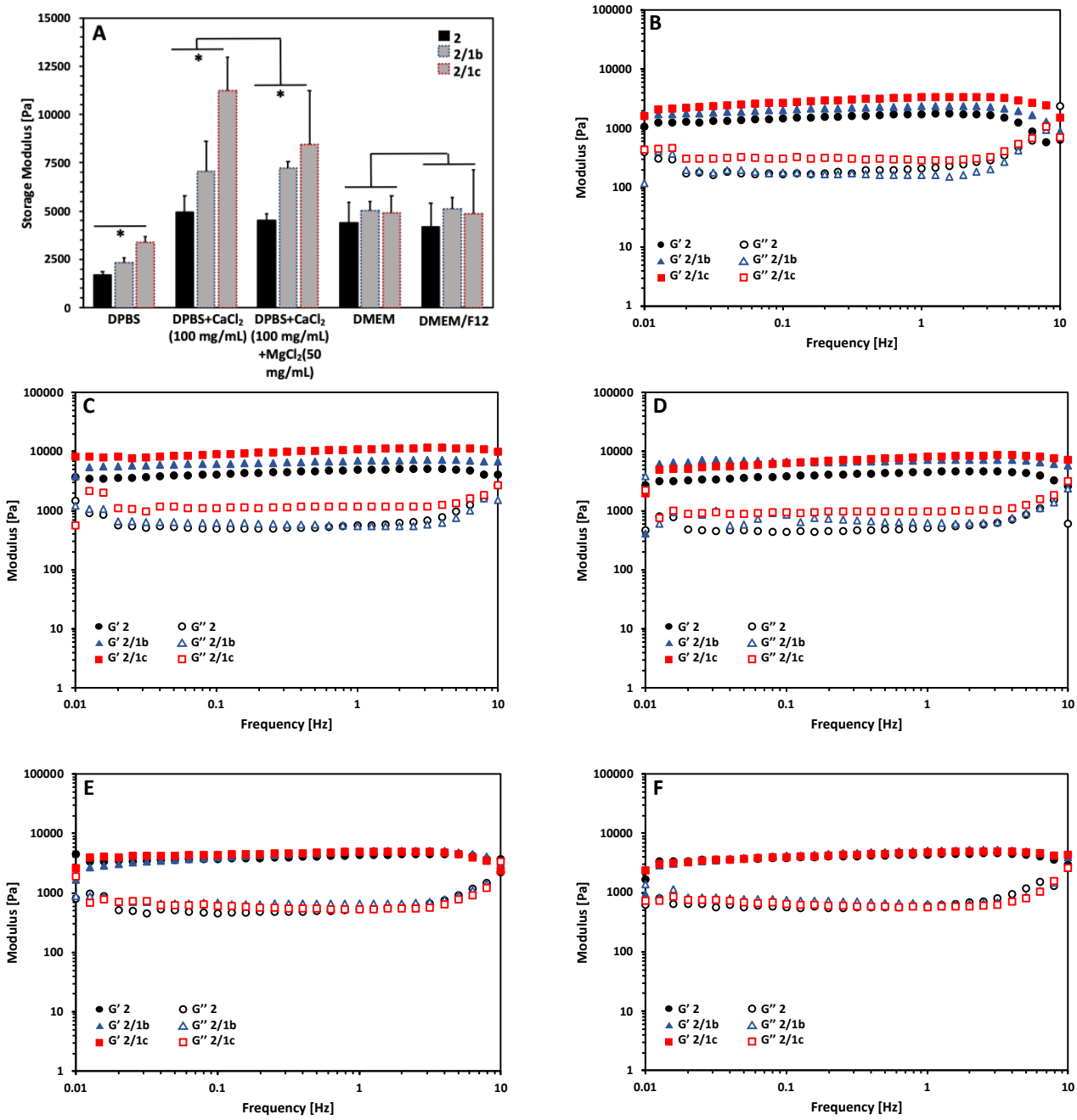


**Figure S23.** Storage modulus of supramolecular gels obtained in different media (A) and representative rheological data for elastic (G') and viscous (G'') moduli in (B) Dulbecco's Phosphate Buffered Saline (DPBS); (C) DPBS supplemented with $CaCl_2$ (100 mg/mL); (D) DPBS supplemented with $CaCl_2$ (100 mg/mL) and $MgCl_2$ (50 mg/mL); (E) Dulbecco's Modified Eagle's Medium (DMEM) supplemented with Fetal Bovine Serum (FBS) at 10%; (F) DMEM-F-12 supplemented with FBS (10%). The same amphiphiles concentration, namely Fmoc-FF (**2,** 10 mM); Fmoc-FF/Fmoc-GlcN6S (**2/1b,** 10 mM/5 mM), and Fmoc-FF/Fmoc-GlcN6P (**2/1c,** 10 mM/5 mM) was used at all conditions. DPBS was chosen because it does not contain divalent cations. The concentration of $CaCl_2$ and $MgCl_2$ was chosen based on the concentration of $Ca^{2+}$ and $Mg^{2+}$ in DMEM.

**S4.3. Interactions of supramolecular gels with basic fibroblast growth factors (FGF-2)**

Among the growth factors, we have selected FGF-2 as it interacts specifically with sulfated glycosaminoglycans. Recombinant human FGF-2 (AF-100-18B) and human FGF-2 enzyme-linked immunosorbent assay development kit (ELISA, 900-K08) were purchased from Peprotech. FGF-2 Antibody (anti-FGF-2), clone bFM-2, 17.5 kDa was purchased from Milipore (05-118).

FGF-2 (1 μg/mL) was added to the solutions of Fmoc-FF, Fmoc-FF/Fmoc-GlcN6S and Fmoc-FF/Fmoc-GlcN6P prior to gelation. The FGF-2 containing solutions (500 μL) were dropped into transwell cell culture inserts (12 wells, Greiner Bio-one) and 1.5 mL of cell culture medium (Dulbecco's Modified Eagle's Medium, DMEM, Sigma) was added to the well and allowed gelation to occur (2 h). The culture medium was changed and this time point was set as 0. The release of FGF-2 was followed by taking aliquots at different time points (2 h, 24 h, 48 h, 72 h and 7 days) and analyzing the solutions by ELISA following the instructions of the supplier. FGF-2 remaining in the hydrogel was quantified by SDS-PAGE & Western Blot. The gels were frozen at -80 °C for 24 h. After this time, they were destroyed by mechanical force: pipetting up and down until a clear solution was obtained. An aliquot of 20 μL was taken from this solution and boiled in Laemmli buffer. The samples were electrophoretically resolved on 12.5% reducing SDS-PAGE. Proteins were transferred to nitrocellulose membranes (Amersham) using a Pierce Power Station and blocked with 5% dry milk in TBS containing 0.1% Tween-20 (TBS-T). The membranes were then incubated at 4 °C with the FGF-2 antibody overnight, followed by alkaline phosphatase-conjugated goat anti-mouse IgG (Vector) for 1 h. After each antibody incubation, the membranes were washed with TBS-T. Signals were developed with the Novex AP chromogenic substrate (Invitrogen).

The distribution of the FGF-2 within the gels was visualized by confocal laser scanning microscope (Leica TCS SP8, Leica Microsystems). The hydrogels were permeabilized with Triton (1%), washed (PBS) and then incubated with anti-FGF-2 (1:200, 1 h, room temperature). After washing (PBS), the gels were stained with AlexaFluor 488 anti-mouse goat (1:500, 1h, room temperature), washed (PBS) and observed under the microscope.

**S4.4 Determination of thermal stability of FGF2 by enzyme-linked immunosorbant assay (ELISA)**

The stability of FGF2 in culture medium at 37 ºC was assessed by a human FGF2 standard ABTS ELISA development kit (PreproTech, UK), according to the manufacture's protocol.

Briefly, 100 µL/well of 1 µg/mL antiFGF2 was immobilized on a 96-well polystyrene plate (E&K Scientific, Campbell, CA) by incubation at room temperature overnight. The plate was then washed 4 times with phosphate buffer saline (PBS) with 0.05% Tween-20 using 300 µL/well. Next, we added 300 µL/well of block buffer (PBS with 1% BSA) and incubated the plate for 1 h at room temperature, followed by washing with PBS. The FGF2 (4ng/mL) was dissolved in DMEM and incubated at 37 ºC. Aliquots of 100 µL were taken at predetermined times, added to microtiter plate and incubated at room temperature for 2 h. After washing, 100 µL/ well of biotinylated Rabbit anti-human bFGF supplemented with D-mannitol was added and incubated for another 2 h. The plate was washed and 100 µL of avidin-anti-bFGF were added to each well and incubated for 30 min. After washing, 100 µL of ABTS substrate solution (Sigma) was added to each well, and incubated at room temperature for color development. The plate was then read at 405 nm with wavelength correction set at 650 nm. The obtained values were used to calculate the concentration of the bioactive FGF2 from a standard curve.

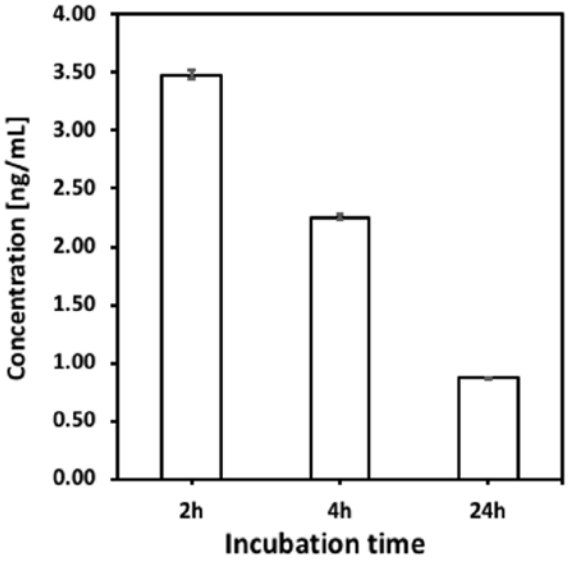


**Figure S24.** FGF-2 is thermally instable and loses most of its activity 24h after incubation at 37 °C as demonstrated by ELISA assay.

**S4.5. Cytotoxicity of the supramolecular gels**

The cytotoxic effect of the gels was evaluated by two different protocols for 2D and 3D cell culture. Under each protocol we assayed three cell lines, namely the fibroblast cell line L929 that is recomended by ISO 109993-5 for testing in vitro cytotoxicity of medical devices; the chondrogenic cell line ATDC5 as we envision soft tissue engineering as possible application of the developed gels; and HeLa as a model for cancer cells. Each cell line was cultured (5% $CO_2$ incubator at 37 °C) on tissue culture polystyrene (TCPS) using the recommended medium (DMEM Low Glucose for L929; DMEM-F12 for ATDC5; and DMEM High Glucose for HeLa) supplemented with 10% fetal bovine serum and 1% Antibiotic/Antimycotic. Upon reaching confluence, the cells were detached from the TCPS with TrypLe (ThermoFisher Sci), centrifuged, and resuspended in the respective medium.

2D cell culture: The cell media and pregelation solutions were heated (water bath) to 37 °C. The gels were formed as described in S4. After gelation the DMEM was replaced by the specific medium (DMEM Low Glucose, DMEM-F12, or DMEM High Glucose) supplemented with 10% fetal bovine serum and 1% Antibiotic/ Antimycotic). This process was repeated 3 times during 24 h to ensure total replacement of the medium. After this period, the top medium from the insert was replaced with a suspension of the respective cell line (L929, ATDC5 or HeLa) at a concentration of $10^5$ cells/gel). The medium was exchanged after 24 h of culture. After 48 h in culture, gels were washed with PBS and incubated with Calcein-AM (Life Technologies) and Ethidium Homodimer-1 (EthE-1, Sigma) in PBS for 10 min. The samples were washed and observed using confocal laser scanning microscope (Leica TCS SP8) with 488 nm (green, Calcein AM) and 633 nm lasers (red, EthE-1).

3D cell culture: pregelation solution (500 μL) was pipetted into transwell cell culture insert, placed into 12 wells culture plate and 1.5 mL of specific cell culture medium (DMEM Low Glucose, DMEM-F12 or DMEM High Glucose) was added in the well (i.e. no medium was added directly to the pregelation solution). The plate was placed in an incubator (5% $CO_2$, 37°C) for 15 min. After this period, the pregelation solution in the insert was mixed (pipetting up and down several times) and the media from the plate was replaced. This process was repeated 3 times. Cell suspension (150 μL, $2.5\times10^5$ cells/gel) was then added into the insert (pipetting up and down several times to mix well) and the plate was incubated again. After gelation (2 h) the media from the bottom of the insert was replaced and 200 μL of fresh medium was added on top of the gel. The medium was exchanged after 24 h of culture. After 48 h in culture, the gels were processed as described above for the 2D culture.

Cell viability: The cell viability was quantified with CellProfiler image analysis software (version 3.0)[4] using the confocal images (at least three per sample) of a live/dead staining. Live cells (green signal) and dead cells

(red signal) were separated from the background using Otsu threshold method and the clumped cells were separated by shape.[5] Cells that were stained simultaneously in green and red were counted as death cells. The cell viability is presented as percentage of live cells from the total of number of cells.

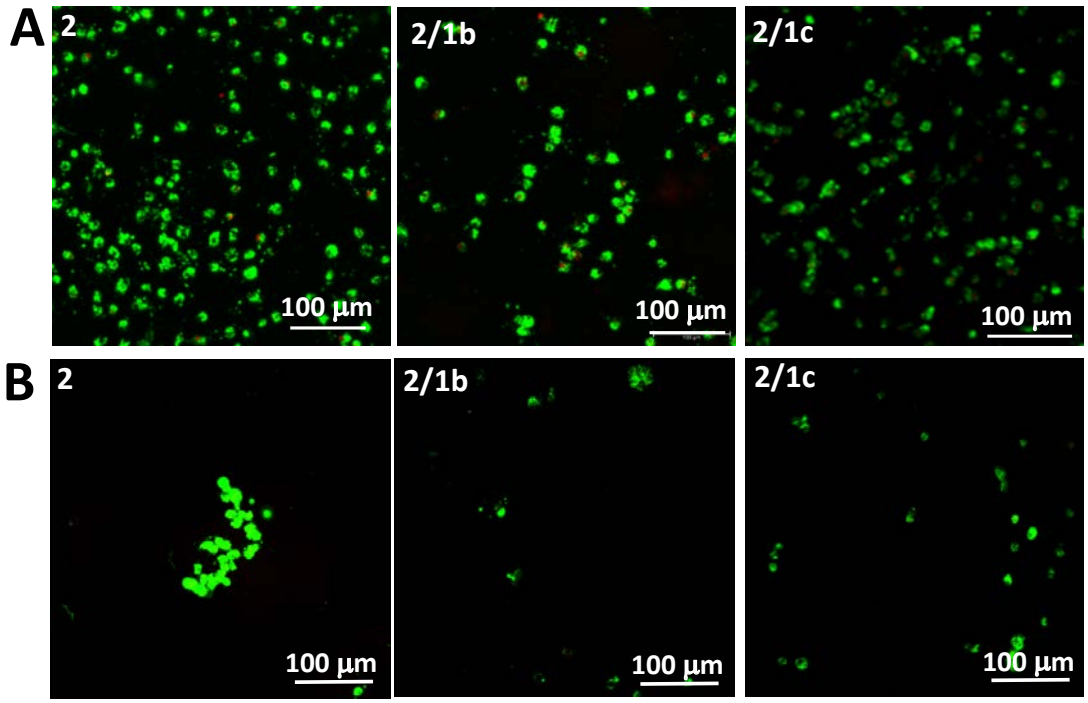


**Figure S25.** Representative laser scanning confocal microscope images of ATDC5 cells cultured (A) on top or (B) encapsulated within the gels for 48 h. Live cells are stained in green and dead ones in red.

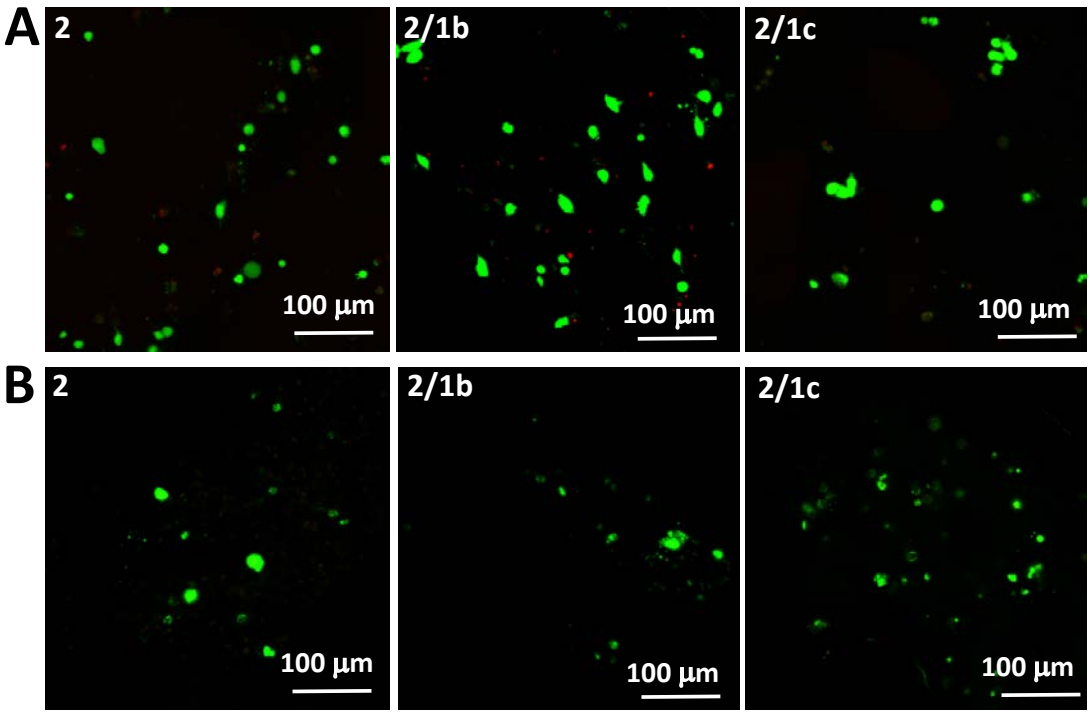


**Figure S26.** Representative laser scanning confocal microscope images of HeLa cells cultured (A) on top or (B) encapsulated within the gels for 48 h. Live cells are stained in green and dead ones in red.

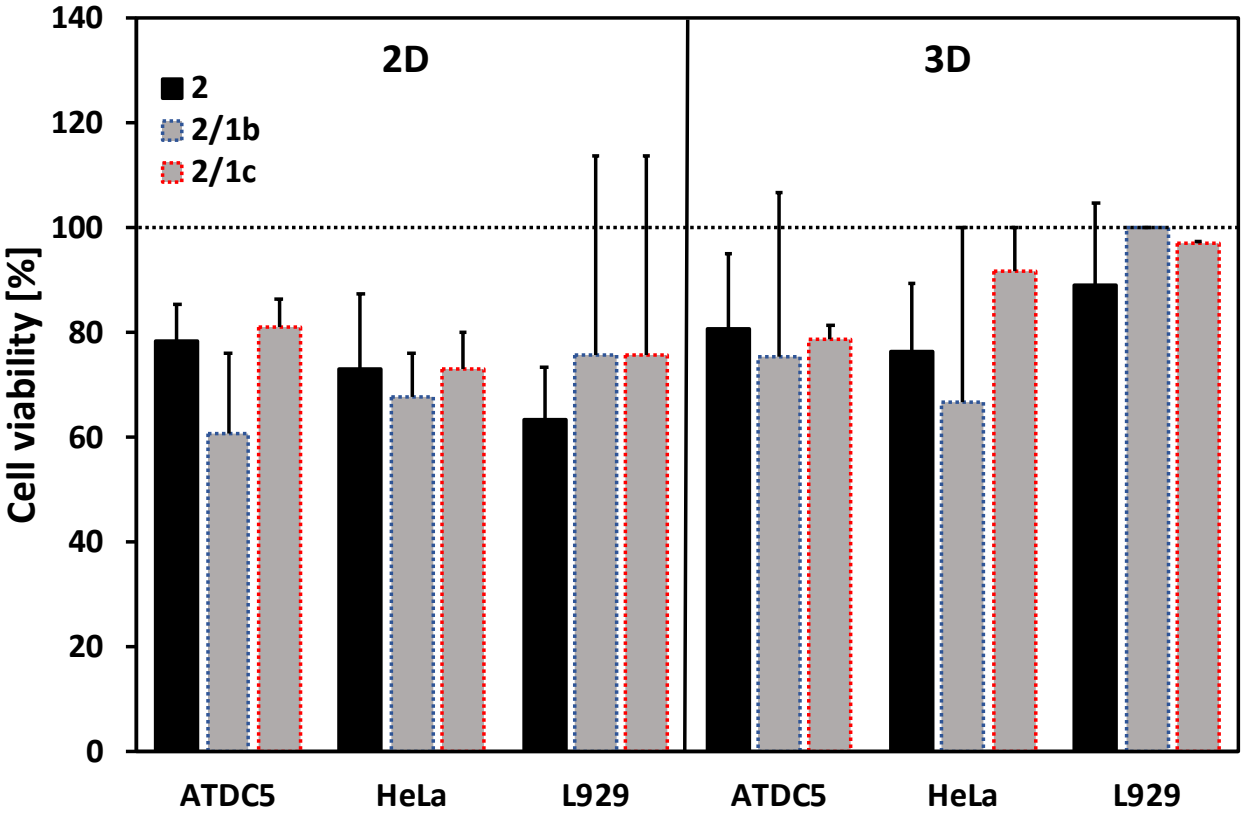


**Figure S27.** Percentage of live cells cultured on top (2D) or encapsulated within the gels (3D) for 48 h.

**References:**


1. R. A. Pires, Y. M. Abul-Haija, D. S. Costa, R. Novoa-Carballal, R. L. Reis, R. V. Ulijn and I. Pashkuleva, *Journal of American Chemical Sociaty*, 2015, **137**, 576-579.
2. L. S. Birchall, S. Roy, V. Jayawarna, M. Hughes, E. Irvine, G. T. Okorogheye, N. Saudi, E. De Santis, T. Tuttle, A. A. Edwards and R. V. Ulijn, *Chem Sci*, 2011, **2**, 1349-1355.
3. V. Jayawarna, M. Ali, T. A. Jowitt, A. E. Miller, A. Saiani, J. E. Gough and R. V. Ulijn, *Adv Mater*, 2006, **18**, 611-614.
4. A. E. Carpenter, T. R. Jones, M. R. Lamprecht, C. Clarke, I. H. Kang, O. Friman, D. A. Guertin, J. H. Chang, R. A. Lindquist, J. Moffat, P. Golland and D. M. Sabatini, *Genome Biol*, 2006, **7**.
5. M. Sezgin and B. Sankur, *J Electron Imaging*, 2004, **13**, 146-168.